International Journal of Engineering and Technology Innovation, vol. 8, no. 2, 2018, pp. 133 - 145

Multi-Response Optimization of Wire Electrical Discharge Machining for Titanium Grade-5 by Weighted Principal Component Analysis

Sachin Ashok Sonawane[1,*], M. L. Kulkarni[2]

[1]Department of Mechanical Engineering, Walchand Institute of Technology, Solapur 413006, Maharashtra, India.

[2]Department of Mechanical Engineering, Rajarshi Shahu School of Engineering and Research, Narhe, Pune 411041, Maharashtra, India.

Received 26 March 2017; received in revised form 06 September 2017; accepted 15 September 2017

Abstract

This paper reports the results of research to examine the effects of cutting parameters such as pulse-on time, pulse-off time, servo voltage, peak current, wire feed rate and cable tension on surface finish, overcut and metal removal rate (MRR) during Wire Electrical Discharge Machining (WEDM) of grade-5 titanium (Ti-6Al-4V). Taguchi's L_{27} orthogonal design method is used for experimentation. Multi-response optimization is performed by applying weighted principal component analysis (WPCA). The optimum values of cutting variables are found as a pulse on time 118 µs, pulse off time 45 µs, servo voltage 40 volts, peak current 190 Amp. , wire feed rate 5 m/min and cable tension 5 gram. On the other hand, Analysis of Variance (ANOVA), simulation results indicate that pulse-on time is the primary influencing variable which affects the response characteristics contributing 76.00%. The results of verification experiments show improvement in the value of output characteristics at the optimal cutting variables settings. Scanning electron microscopic (SEM) analysis of the surface after machining indicates the formation of craters, resolidified material, tool material transfer and increase in the thickness of recast layer at higher values of the pulse on time.

Keywords: WEDM, titanium grade-5, Taguchi method, weighted principal component analysis, ANOVA, SEM analysis

1. Introduction

Titanium is the ninth most abundant available element in the earth's crust and mostly used as a structural metal and exotic space-age metal. Titanium and its alloys possess high strength, minimum weight ratio, low density, exceptional corrosion resistance, excellent properties at elevated temperature, a low thermal coefficient of expansion, non-magnetic, high fracture toughness and fatigue strength, excellent cryogenic properties, great ballistic resistance-to-density ratio and non-hazardous, non-allergenic and are completely biocompatible. Due to these features, they find broad applications in the biomedical field, aerospace, chemical industry, power generation, oil and gas extraction, automotive, sports, etc.

High cutting temperatures up to even 1100°C is produced in the proximity of cutting periphery of the tool while machining of titanium alloys. As titanium alloys possess very low thermal conductivity, nearly 80% of the heat produced, is conducted into the tool which results in rapid wear of the tool. Titanium alloys offer high resistance to its deformation at elevated temperature and due to the minimal area of contact between chip and tool on the rake face generates higher mechanical stresses in the adjacent area of the cutting edge which is generally three to four times more than that of nickel alloys and steels. Due to low elasticity modulus, chatter is another major problem involved during finish machining of

* Corresponding author. Email address: sonawanesachin09@gmail.com

Tel.: +91-9850959863

titanium alloys. While machining, deflection of titanium is twice than that of carbon steel, resulting in springing back action behind the cutting edge of the tool. This bouncing motion on the cutting areas leads to impulsive flank wear, vibration and cutting temperature increase. When cutting temperature exceeds 500°C, titanium and its alloys exhibit high chemical reactivity with cutting tool materials. While machining of titanium, chips pressure welds to the cutting tool which results in dissolution-diffusion wear and increases as temperature rises [1]. These problems can be minimized by utilizing non-traditional machining process such as Wire Electrical Discharge Machining (WEDM).

WEDM is a thermal energy cutting process, where material removal mechanism is mainly due to melting and vaporization effect and takes place by heat generated with incessant discrete sparks produced in a small gap between wire and workpiece in existence of dielectric fluid. WEDM technology is widely used in conductive materials machining mainly for the production of mold, dies, medical and dental instrumentation, graphite electrodes, parts in automotive and aerospace industries [2].

Liao [3] used the weighted principal component (WPC) technique for three different case studies and found that WPC method is advantageous than principal component analysis (PCA) and Taguchi method. Gauri and Chakraborty [4] applied WPC method for various case studies and concluded that WPC method eliminates uncertainty in the decision-making process in the selection of weights for different characteristics which is associated with other methods. Routara et al. [5] used WPCA method for optimization during cylindrical grinding of UNS C34000 brass. Biswas et al. [6] attempted sub-merged arc welding (SAW) of mild steel plates and implemented WPCA method for the optimization of bead height, width, heat affected zone (HAZ) and penetration depth. Padhi et al. [7] performed WEDM on EN 31 steel. For the optimization of dimensional deviation, MRR and surface roughness Taguchi system integrated with PCA was used. Zhao et. al. [8] carried out spot welding of TC2 titanium alloy sheets to study the effect of welding parameters on various welding quality characteristics and optimized them with the help of PCA. Das et al. [9] performed multi-feature optimization by using WPCA during EDM of EN-31tool steel. Taguchi's L27 orthogonal design was used to find out the influence of Ton, Toff, IP, and SV on MRR and surface roughness. Rao and Krishna [10] used an integrated approach principal component analysis coupled with Taguchi method for the optimization of the process parameters during machining of ZC63/SiCp MMC. Gauri and Pal [11] discussed some limitations while applying PCA-related methods for multi-characteristics optimization. Soepangkat and Kis Agustin [12] carried out operations on SKD61 tool steel on WEDM and used WPCA for the optimization of surface roughness and recast layer thickness. Mohanty et al. [13] used WPCA integrated with Taguchi method for the optimization of control parameters during EDM of D2 steel. Panda et al. [14] performed turning tests on EN 31 steel and used WPCA method for the optimization of different values of surface roughness. Lusi et al. [15] presented experiments on H 13 tool steel using WEDM. For the optimization of MRR and surface roughness, both Taguchi and WPCA method was utilized. Costa et al. [16] conducted end milling operations on AISI 1045 steel in a dry environment. For the optimization of SR and MRR, a combination of WPCA and S/N ratio was used. Dhakad and Vimal [17] performed operations on EN45 alloy steel on WEDM. Taguchi technique combined with PCA method was used for the optimization of machining time, MRR and gap voltage. Nair and Kumanan [18] performed abrasive water jet machining (AWJM) on Inconel 617. WPCA technique was applied for the optimization of MRR, parallelism, circularity, perpendicularity, and cylindricity of the cut profiles.

In this research, tests are conducted on Ti-6Al-4V using six control factors of WEDM. Taguchi's L27 experimental design is used to perform the trials. Three quality characteristics selected for the study are surface roughness, overcut and MRR. WPCA technique is applied to convert multi-response optimization problem into an equivalent single quality response known as the multi-response quality index (MQI). The optimal levels of the control parameter are then determined at which more substantial value of MQI is present. Since larger the MQI better is the quality. Finally, verification trials are performed to confirm the results. SEM analysis of the cut surfaces is carried out to examine the various aspects of the surface integrity.

Copyright © TAETI

2. Experimentation

2.1. Test set up and work material

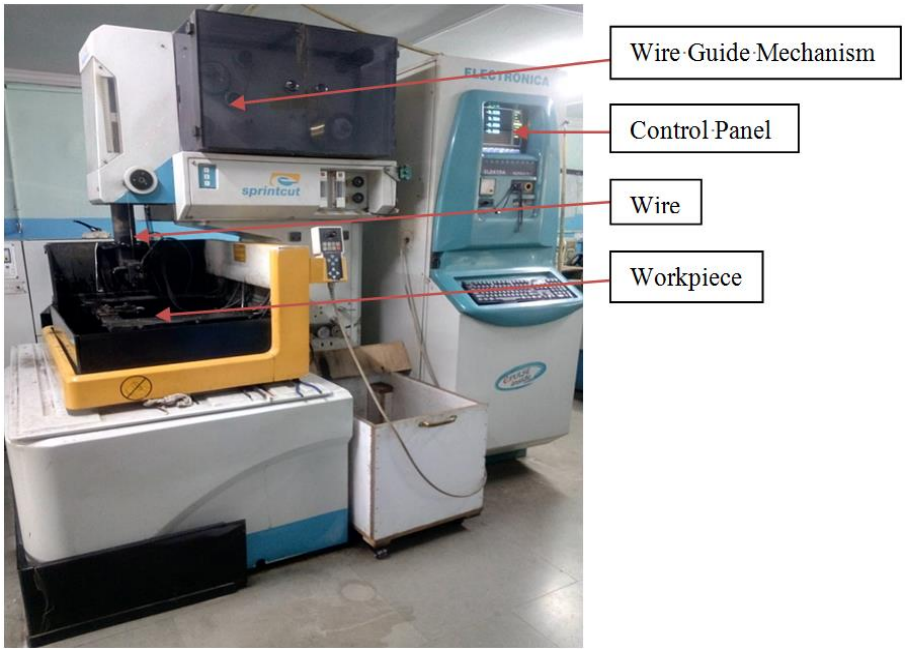

Fig. 1 ePULSE-40 sprint cut WEDM

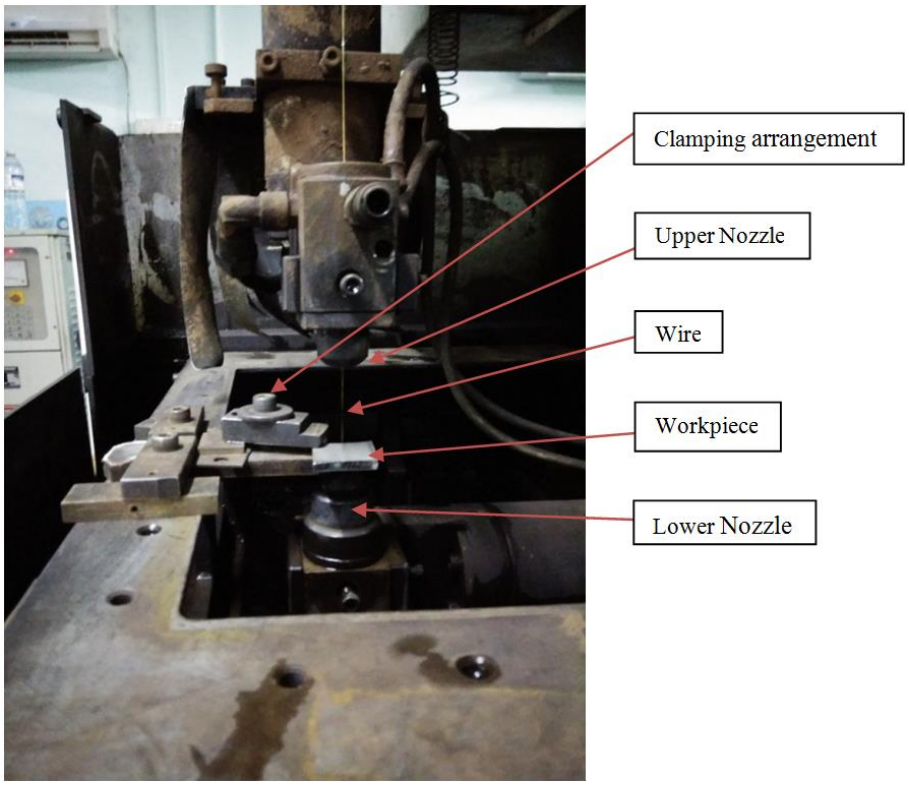

Fig. 2 Experimental setup

A series of trials are performed on ePULSE-40 5-axis sprint cut WEDM manufactured by Electronica Machine Tool Ltd., India (Fig. 1) to acquire the data for modeling. Fig. 2 shows the details of the experimental setup. The material applied to the investigation is Titanium grade-5 of size 30 mm x 30 mm x 5 mm thick which is connected to the negative polarity. The chemical composition of the material is 6 wt. % Al, 4 wt. %V, 0.25 wt.% (max) Fe, 0.2(max) wt.% O and remainder titanium. The brass wire of 0.25 mm diameter with positive polarity is used to cut a block of 10 mm x 10 mm x 5 mm thickness. De-ionized water is used as a dielectric with a flushing pressure of 15 kg/cm^2 to flush out the debris from the

Copyright © TAETI

cutting zone. The conductivity of the dielectric is maintained at a constant value of 20 µS/cm at 22°C.Trials are performed with zero wire offset. The value of servo feed is kept at 2120 units.

2.2. Measurement of quality features

There are various machining features that are associated with the WEDM process which must be optimized for better performance and economy. In the present study, various machining characteristics are studied. These are discussed as follows:

2.2.1. *Metal removal rate (MRR)*

MRR is computed by measuring the weight of the workpiece before and after machining divided by cutting time. The weight of the workpiece is measured with an electronic weighing balance (Fig. 3) having an accuracy of 0.01 gm. The computed weight loss is then transformed into the volume of material removed in mm^3/min using the Eq. (1).

$$\text{MRR} = \frac{Volume\ of\ material\ removed}{Time\ taken\ in\ min} \tag{1}$$

Fig. 3 Measurement of weight by using an Electronic weigh balance

2.2.2. *Surface finish*

The surface finish of the square block is measured in µm by using a Mitutoyo make digital surface tester SJ-210 (Fig.4). The surface finish is measured three times on each machined surface perpendicular to the cut, and then an average is made. The cut off length is selected as 0.8 mm during measurement.

Fig. 4 Surface roughness measurement using surface tester SJ-210

Copyright © TAETI

2.2.3. Overcut

Overcut [19] is calculated by using the Eq. (2).

$$\text{Overcut} = \frac{Size\ of\ cut - d}{2} \tag{2}$$

where d = Diameter of wire in mm

The size of the cut is the algebraic difference of dimensions between the square block and square on the workpiece.

The dimension of the square block is assessed with a digital micrometer (Mitutoyo, 1 micron, Fig. 5) and the size of the square on the workpiece is measured by a profile projector (Dr. Heinrich Schneider - ST 360 H, 0.1 micron, Fig. 6).

Fig. 5 Measurement of a square block using digital micrometer

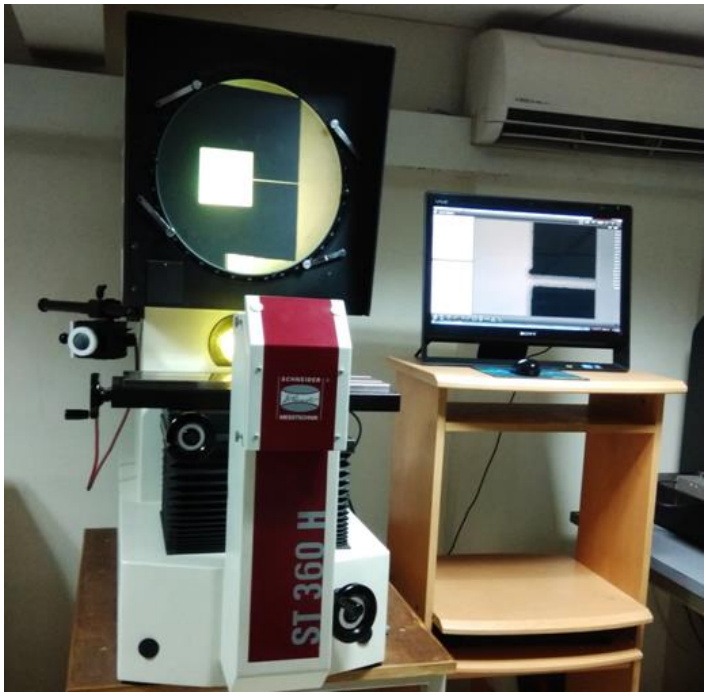

Fig. 6 Dr. Heinrich Schneider ST 360 H profile projector

2.3. Plan of experiments

In the present study, six cutting variables are considered such as pulse-on time (T_{ON}), pulse-off time (T_{OFF}), servo voltage (SV), peak current (IP), wire feed rate (W_F), and cable tension (W_T). Initially, pilot stage experiments are realized by changing one variable at a time while keeping other variables constant at some value to detect the ranks of each cutting variable. Table 1 presents the levels of the cutting factors used during experimentation. Taguchi's L_{27} experimental design is used for testing, and each trial run is realized thrice thus 81 experiments total. The response characteristics preferred for the present study are surface roughness, overcut and MRR. Table 2 presents the results of Taguchi method.

The S/N ratio of surface roughness and overcut is calculated considering "lesser-the-better" attribute and for MRR "higher-the-better" feature is used as presented by Eqs. (3) and (4), respectively.

Copyright © TAETI

$$\zeta_{LB} = -10 \log \left[\frac{1}{n}\sum_1^n Kxy^2\right] \quad (3)$$

$$\zeta_{HB} = -10 \log \left[\frac{1}{n}\sum_1^n 1/Kxy^2\right] \quad (4)$$

where K_{xy} is the x^{th} experimental value at the y^{th} test and n is the total number of repetitions.

Software used for the statistical analysis is Minitab 16.

Table 1 Cutting variables and their ranks

Symbol	Cutting Parameter	Unit	Level 1	Level 2	Level 3
T_{ON}	Pulse on Time	µs	110	114	118
T_{OFF}	Pulse off Time	µs	45	50	55
SV	Servo Voltage	Volts	20	30	40
IP	Peak Current	Amp	170	190	210
W_F	Wire Feed Rate	m/min	1	3	5
W_T	Cable Tension	Gram	2	5	8

Table 2 Taguchi's L_{27} orthogonal arrangement along with response features

Expt. No.	T_{ON}	T_{OFF}	SV	IP	W_F	W_T	Surface Roughness (µm)	Overcut (mm)	MRR (mm^3/min)
1	110	45	20	170	1	2	1.82	0.294	21.00
2	110	45	20	170	3	5	1.68	0.225	18.26
3	110	45	20	170	5	8	1.60	0.247	17.80
4	110	50	30	190	1	2	1.76	0.310	20.16
5	110	50	30	190	3	5	1.70	0.220	18.76
6	110	50	30	190	5	8	1.61	0.272	17.72
7	110	55	40	210	1	2	1.79	0.276	20.54
8	110	55	40	210	3	5	1.58	0.298	17.50
9	110	55	40	210	5	8	1.52	0.164	17.06
10	114	45	30	210	1	5	2.32	0.274	28.23
11	114	45	30	210	3	8	2.19	0.251	27.69
12	114	45	30	210	5	2	1.85	0.163	22.00
13	114	50	40	170	1	5	2.28	0.185	28.03
14	114	50	40	170	3	8	1.79	0.176	20.60
15	114	50	40	170	5	2	2.01	0.172	24.87
16	114	55	20	190	1	5	1.95	0.262	23.57
17	114	55	20	190	3	8	2.06	0.161	25.70
18	114	55	20	190	5	2	1.97	0.157	24.65
19	118	45	40	190	1	8	2.51	0.282	32.20
20	118	45	40	190	3	2	2.04	0.168	25.37
21	118	45	40	190	5	5	2.41	0.160	30.54
22	118	50	20	210	1	8	2.10	0.312	27.38
23	118	50	20	210	3	2	2.36	0.265	28.40
24	118	50	20	210	5	5	2.25	0.198	27.79
25	118	55	30	170	1	8	2.50	0.210	31.04
26	118	55	30	170	3	2	2.31	0.159	28.00
27	118	55	30	170	5	5	1.73	0.178	19.20

3. Multi-Response Optimization by WPCA Technique

Principal component analysis (PCA) is a multi-element statistical tool developed by Pearson [20] and Hotelling [21]. This method presents the arrangement of variance-covariance through the linear combinations of all the response characteristics. It converts a set of interrelated response characteristics into an independent primary component. However, in the case of realized research for multi-response optimization WPCA technique is applied. In this method, all the main elements in spite of the eigenvalues are considered; therefore, overall deviation in every character is fully explained. In this technique, weight for each response feature is taken as the amount of total difference contributed by every component to unite the entire principal elements which will appear as a multi-response quality index (MQI). The different steps of WPCA technique are explained below:

Copyright © TAETI

Step I: Compute S/N ratio of each response

S/N ratio for the respective response characteristics is computed by using Eqs. (3) & (4) and are presented in Table 3.

Table 3 S/N ratios and scaled S/N ratios of each response characteristic

Expt. No.	S/N ratios			Scaled S/N ratios		
	Surface Roughness	Overcut	MRR	Surface Roughness	Overcut	MRR
1	-4.8940	10.6328	26.4160	0.567935	0.077296	0.321761
2	-3.6947	12.9563	25.2297	0.798902	0.467558	0.106692
3	-3.2694	12.1573	25.0082	0.880809	0.333356	0.066535
4	-4.4890	10.1726	26.0912	0.645932	0	0.262876
5	-3.9188	13.0854	25.4646	0.755744	0.489242	0.149278
6	-3.2096	11.3086	24.9707	0.892325	0.190806	0.059736
7	-4.5930	11.1712	26.2520	0.625903	0.167728	0.292028
8	-2.9639	10.5059	24.8607	0.939644	0.055982	0.039794
9	-2.6505	15.6845	24.6412	1	0.925794	0
10	-7.1842	11.2555	29.0131	0.126875	0.181887	0.7926
11	-6.7168	11.9949	28.8453	0.21689	0.306079	0.762178
12	-5.0896	15.7385	26.8510	0.530265	0.934864	0.400624
13	-6.9535	14.6555	28.9514	0.171305	0.75296	0.781414
14	-4.7444	15.0724	26.2867	0.596745	0.822984	0.298319
15	-5.6219	15.3061	27.9119	0.427752	0.862237	0.592959
16	-5.3769	11.6450	27.4483	0.474935	0.247308	0.508911
17	-6.0211	15.8812	28.1998	0.350871	0.958832	0.645153
18	-5.4837	16.0798	27.8360	0.454367	0.99219	0.579198
19	-7.8430	10.9949	30.1571	0	0.138116	1
20	-5.8754	15.4762	28.0851	0.378931	0.890807	0.624359
21	-7.4834	15.9155	29.6964	0.069254	0.964593	0.916478
22	-6.3908	10.1261	28.7476	0.279673	-0.00781	0.744466
23	-7.2746	11.5459	29.0653	0.109466	0.230663	0.802063
24	-6.8354	14.0812	28.8777	0.194049	0.656499	0.768052
25	-7.7125	13.5690	29.8375	0.025132	0.570469	0.942058
26	-7.1216	15.9900	28.9421	0.138931	0.977107	0.779728
27	-4.1736	15.0075	25.6684	0.706673	0.812083	0.186225

Step II: Compute scaled S/N ratios of each response characteristic

In this step scaled S/N ratios are calculated for each response characteristic in the range of 0 to 1 using Eq. (5). This will reduce the inconsistency between the values of different response characteristics.

$$M_{XY} = \frac{\zeta xy - \min \zeta y}{\max \zeta y - \min \zeta y}, \ for \ (x = 1, 2, 3, ..., m; \ y = 1, 2, 3, ..., n) \tag{5}$$

where, M_{xy}= value of scaled S/N ratio for y^{th} response at x^{th} experimental run, min ζ_y= min (ζ_{1y}, ζ_{2y}, ζ_{3y}, ….,ζ_{my}) and max ζ_y= max (ζ_{1y}, ζ_{2y}, ζ_{3y}, …., ζ_{my}).

The scaled S/N ratios of each response characteristics are represented by a matrix as shown below by Eq. (6):

$$M = \begin{pmatrix} M_1(1) & M_1(2) & M_1(3) & ... & M_1(v) \\ M_2(1) & M_2(2) & M_2(3) & ... & M_2(v) \\ M_u(1) & M_u(2) & M_u(3) & ... & M_u(v) \end{pmatrix} \tag{6}$$

where u= experimental runs = 27, v = number of response characteristic= 3.Scaled S/N ratios are calculated for each response characteristic and are shown in Table 3.

Copyright © TAETI

Step III: Correlation coefficient matrix

The correlation coefficient matrix is estimated as given by Eq. (7):

$$A_{yp} = \left(\frac{Cov(\mathrm{Mu}(y), \mathrm{Mu}(p))}{\sigma(\mathrm{Mu})(\mathrm{y}) \text{ x } \sigma(\mathrm{Mu})(\mathrm{p})} \right),\ y = 1, 2, 3, ...,\ n;\ p = 1, 2, 3, ...,\ n \tag{7}$$

where Cov ($M_u(y)$, $M_u(p)$) is the covariance of sequences $M_u(y)$ and $M_u(p)$, $\sigma_{(Mu)}(y)$ is the standard deviation of sequence $M_u(y)$ and $\sigma_{(Mu)}(p)$ is the standard deviation of sequence $M_u(p)$.

Step IV: Eigenvalues and eigenvectors calculation

From the correlation coefficient matrix, eigenvalues and eigenvectors are determined by Eq. (8) as follows:

$$(A - \lambda_s I)Q_{sk} = 0 \tag{8}$$

where λ_s = eigenvalues and $\sum_{s=1}^{n} \lambda s = n$, $s = 1,2,3,\ldots,n$; $Q_{sk} = [b_{k1} b_{k2} \ldots\ldots b_{kn}]^{\mathrm{T}}$ = eigenvectors related to the eigenvalues λ_s. Table 4 shows eigenvalues, eigenvectors, and explained variation of each response characteristic.

Table 4 Correlation matrix with Eigen values, Eigen vectors and explained variation

Principal Component	Eigenvalue	Eigenvector	Amount of explained Variation
First	2.0203	[-0.696 (b_{11}), 0.169 (b_{12}), 0.698 (b_{13})]	0.673 (ξ_1)
Second	0.9704	[0.132 (b_{21}), 0.986 (b_{22}), -0.107 (b_{23})]	0.323 (ξ_2)
Third	0.0092	[0.706 (b_{31}), 0.169 (b_{32}), 0.698 (b_{33})]	0.003 (ξ_3)

Step V: Determination of principal components

The h^{th} primary component about u^{th} experimental run can be calculated as represented by Eq. (9):

$$Z_h^{\,i} = b_{h1}M_{u1} + b_{h2}M_{u2} + \ldots\ldots + b_{hp}M_{up};\ (h = 1,2,3,\ldots,\ p) \tag{9}$$

The principal component for each response characteristic i.e. surface roughness, overcut and MRR is computed by using following Eqs. (10), (11) & (12) and are presented in Table 5.

$$Z_1^{\,i} = -0.696\ M_{u1} + 0.169\ M_{u2} + 0.698\ M_{u3} \tag{10}$$

$$Z_2^{\,i} = 0.132\ M_{u1} + 0.986\ M_{u2} - 0.107\ M_{u3} \tag{11}$$

$$Z_3^{\,i} = 0.706\ M_{u1} - 0.017\ M_{u2} + 0.708\ M_{u3} \tag{12}$$

Step VI: Calculate multi-response quality index (MQI) for each experiment

Multi-response quality index (MQI) represents weighted sum of all the principal components. MQI value for i^{th} experimental run therefore may be computed using the Eq. (13).

$$MQI = \sum_{(h=1)}^{p} \xi_i Z_h^{\,i} \tag{13}$$

where ξ_i is the amount of overall variance of the response characteristics explained by the h^{th} principal component, $Z_h^{\,i}$ is the calculated value of h^{th} primary component about i^{th} experimental run and $\sum_{h=1}^{p} \xi_i = 1$. Larger the value of MQI better will be the quality.

$$\mathrm{MQI}^i = 0.673\ Z_1^{\,i} + 0.323\ Z_2^{\,i} + 0.003\ Z_3^{\,i} \tag{14}$$

The MQI values for every test is calculated by applying Eq. (14) and indicated in Table 5.

Copyright © TAETI

Table 5 Values of Principal components of all response attributes and Multi-response quality Index (MQI)

Expt. No.	Principal Components			Multi-response quality Index (MQI)	Rank
	Surface Roughness (Z_1^i)	Overcut (Z_2^i)	MRR (Z_3^i)		
1	-0.157630	0.116753	0.627454	-0.066490	22
2	-0.402550	0.555051	0.631614	-0.089740	23
3	-0.510260	0.437836	0.663291	-0.200000	25
4	-0.266080	0.057135	0.642144	-0.158690	24
5	-0.339120	0.566178	0.630927	-0.043460	20
6	-0.547120	0.299530	0.669031	-0.269450	26
7	-0.203450	0.216752	0.645792	-0.064970	21
8	-0.616750	0.174973	0.690611	-0.356490	27
9	-0.539540	1.044833	0.690262	-0.023560	19
10	0.495668	0.111280	0.647642	0.371471	13
11	0.432773	0.248870	0.687543	0.373704	12
12	0.068563	0.948904	0.642116	0.354565	14
13	0.553449	0.681420	0.661382	0.594554	4
14	-0.068020	0.858312	0.618522	0.233311	15
15	0.261888	0.843182	0.707149	0.450720	9
16	0.066460	0.252084	0.691409	0.128225	18
17	0.368153	0.922692	0.688183	0.547861	5
18	0.255721	0.976301	0.713988	0.489588	9
19	0.721342	0.029182	0.705652	0.497006	8
20	0.322613	0.861549	0.694428	0.497482	7
21	0.754517	0.862168	0.681361	0.788314	1
22	0.323665	-0.050440	0.724664	0.203708	16
23	0.522634	0.156063	0.641222	0.404065	11
24	0.511991	0.590741	0.669619	0.537388	6
25	0.736474	0.464999	0.675023	0.647867	3
26	0.612685	0.898335	0.633522	0.704400	2
27	-0.224620	0.874069	0.616953	0.133008	17

Step VII: Optimal arrangement of the cutting variables

Table 6 shows the average values of MQI with respect to different stages of the control parameters. For example, it can be seen from Table 2 that factor T_{ON} is set at rank 1 in the first nine tests and therefore, MQI value at rank 1 of factor T_{ON} is found as the average of the MQI values with reference to the first nine trials. Since, a greater value of MQI indicates better quality. Thus, the optimal setting of the cutting parameters is with pulse on time (T_{ON}) = 118 µs, pulse off time (T_{OFF}) = 45 µs, servo voltage (SV) = 40 volts, peak current (IP) = 190 Amp, wire feed rate (W_F) = 5 m/min and cable tension (W_T) = 5 gram.

Table 6 Average values of MQI for each cutting variable

Level	T_{ON}	T_{OFF}	SV	IP	W_F	W_T
1	-0.1413	0.2807	0.2171	0.2675	0.2391	0.2200
2	0.1313	0.2169	0.2348	0.2752	0.2511	0.2292
3	0.4900	0.2451	0.2907	0.1999	0.2523	0.2233

Step VIII: ANOVA and Verification experiments

ANOVA is performed to establish major influencing factors and percentage contribution of cutting parameters for MQI. The results of ANOVA are represented in Table 7.

The percentage contribution of each cutting variable influencing MQI is shown in Fig. 7. Major noteworthy factor affecting the response characteristics is T_{ON} which contributes 76.00%, followed by IP 11.40%, W_T 6.5%, W_F 1.03%, T_{OFF} 0.67% and SV 0.035%. Three verification trials, at the optimum arrangement of cutting variables, are performed. The results of verification tests are indicated in Table 8.

Copyright © TAETI

Table 7 ANOVA for MQI

Source	DF	Seq SS	Adj MS	F	P	% Contribution
T_{ON}	2	2.08478	1.04239	122.36	0.000*	76.00
T_{OFF}	2	0.01840	0.00920	1.08	0.366	0.67
SV	2	0.00096	0.00048	0.06	0.946	0.03
IP	2	0.31308	0.15654	18.37	0.000*	11.40
W_F	2	0.02833	0.01417	1.66	0.225	1.03
W_T	2	0.17816	0.08908	10.46	0.002*	6.50
Error	14	0.11927	0.00852	-	-	4.35
Total	26	2.74298	-	-	-	-

S = 0.0922999 R-Sq = 95.65% R-Sq(adj) = 91.92%

*P-value < 0.05 indicates significant parameter at 95% confidence level

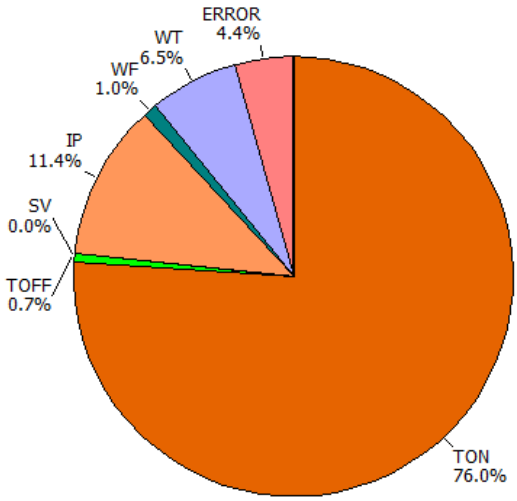

Fig. 7 Percentage contribution of cutting variables on MQI

Table 8 Verification test results at the optimum arrangement of cutting variables

Sr. No.	Response characteristic	Optimum value	
		Predicted value	Experimental value
1	Surface roughness, µm	-	2.26
2	Overcut, mm	-	0.152
3	MRR, mm^3/min	-	34.57
4	MQI	0.788314	0.827157

4. SEM Analysis of Machined Samples

From Fig. 8 to 10, it is observed that at Experiment No. 19 microstructure indicates matt surface, large deep craters, more amount of molten material resolidified on the machined surface in the form of debris and micro-cracks. At high values of the pulse on time, more amount of discharge energy is released for machining. It results in subsequent melting and vaporization of material from the workpiece surface. The surface finish depends upon power contained per spark and efficient utilization of that spark for producing a crater. The higher the pulse on time, the more significant the amount of discharge energy hence more amount of heat is generated and large dark holes are formed on the workpiece surface. Some of the molten material produced by the discharge is carried away by the dielectric. The remaining molten material gets re-solidified to form debris and spherical globules. Micro-cracks are formed due to the existence of thermal stress and tensile stress in the machined workpiece. Thermal stress is created when the sparks hit the cut surface during machining. Tensile stress in the component is produced as some of the molten material is flushed away from the part's surface by the dielectric and some remains resolidified on the surface. As the carbon reacts with molten metal, it bonds more than the natural parent element during the cooling process, and when the stress on the surface surpasses the material's ultimate tensile strength, cracks are formed. From SEM-EDX analysis, it is observed that tool material migrates (traces of Cu & Zn) from wire to the

Copyright © TAETI

workpiece surface the value of which varies from 7.02 wt% at low energy input to 13.98 wt% at high power input. Also, at high values of the pulse on time and lower values of pulse off time, average recast layer thickness increases (>4μm). This is because some amount of molten material does not get flushed away and remains solidified on the surface.

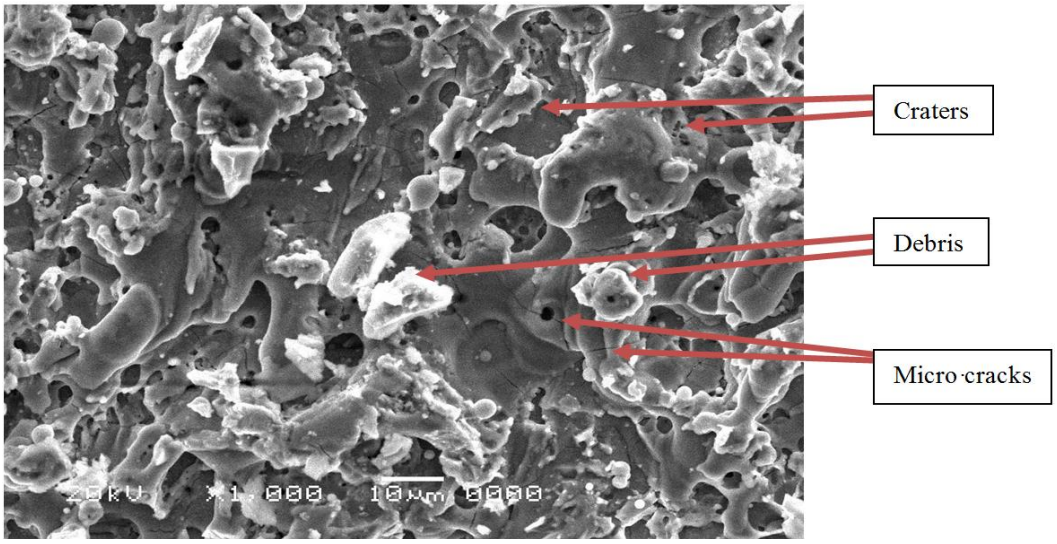

(a) Experiment No. 9 (Low energy input)

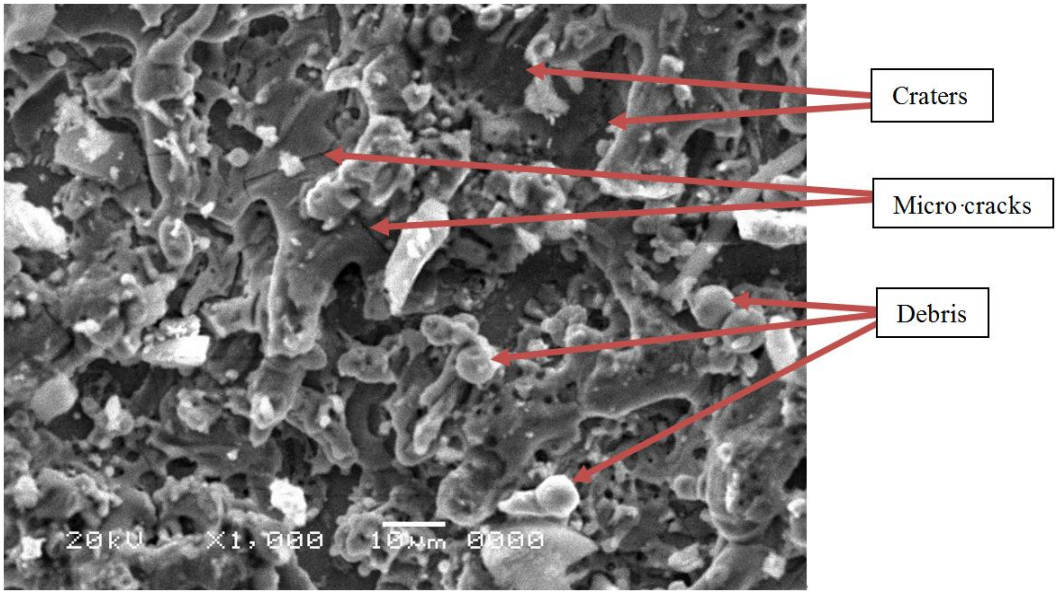

(b) Experiment No. 19 (High energy input)

Fig. 8 Microstructure of Machined samples

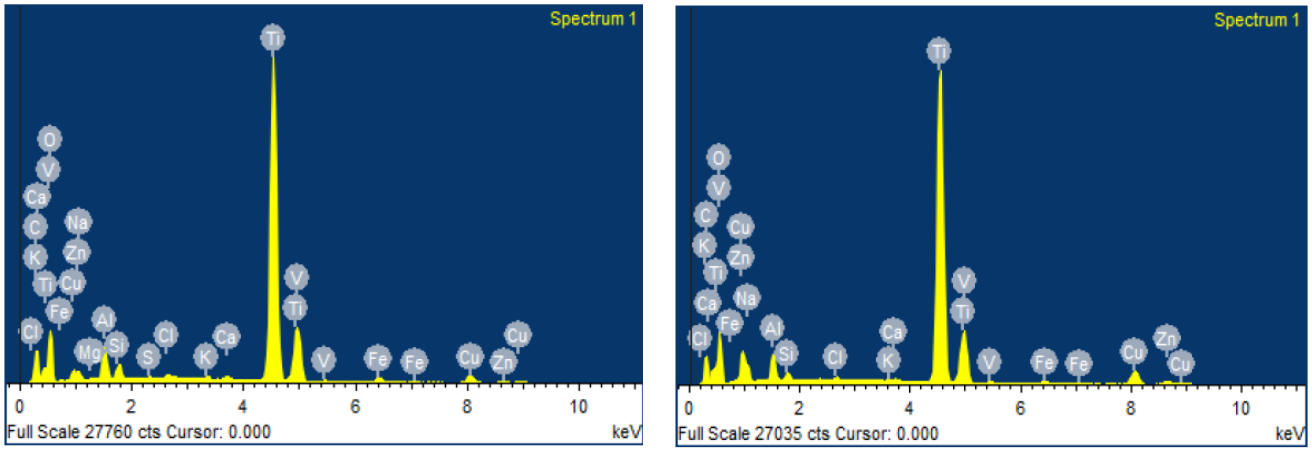

(a) Experiment No. 9 (Low energy input) (b) Experiment No. 19 (High energy input)

Fig. 9 SEM-EDX analysis of machined samples

Copyright © TAETI

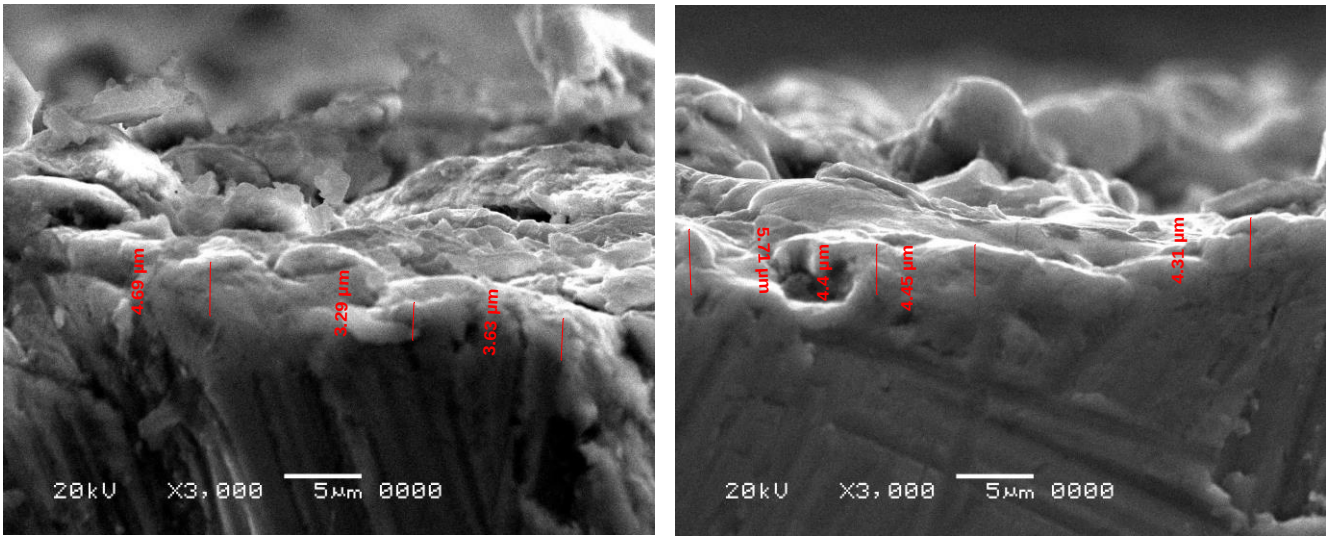

(a) Experiment No. 9 (Low energy input) (b) Experiment No. 19 (High energy input)

Fig. 10 SEM image of recast layer of machined samples

5. Conclusions

WPCA technique is used to detect the optimal arrangement of cutting parameters while machining of Ti-6Al-4V on WEDM. To examine effect of pulse-on time (T_{ON}), pulse-off time (T_{OFF}), servo voltage (SV), peak current (IP), wire feed rate (W_F) and cable tension (W_T) on response characteristics such as surface roughness, overcut and MRR, tests are carried out by applying Taguchi's L_{27} orthogonal plan. From this research, the results are summarized as given below:

(1) Applying WPCA technique, the optimum settings of the cutting parameters which give the highest MQI values as: T_{ON} =118 µS, T_{OFF} = 45 µS, SV = 40 volts, IP = 190 Amp, W_F = 5 m/min and W_T = 5 gram.

(2) Outcomes of the ANOVA specify that T_{ON} contributing 76.00% is the key variable which affects MQI.

(3) SEM analysis of machined samples shows that, at higher values pulse on time surface quality decreases owing to the formation of the major deep craters, more amount of molten material resolidified on the workpiece surface, migration of tool material and increased recast layer thickness.

References

[1] E. O. Ezugwu and Z. M. Wang, "Titanium alloys and their machinability-a review," Journal of Materials Processing Technology, vol. 68, no. 3, pp. 262-274, August 1997.

[2] K. H. Ho, S. T. Newman, and S. Rahimifard, "State of the art in wire electrical discharge machining (WEDM)," International Journal of Machine Tools and Manufacture, vol. 44, no. 12-13, pp. 1247-1259, October 2004.

[3] H. C. Liao, "Multi-response optimization using weighted principal component," International Journal of Advanced Manufacturing Technology, vol. 27, no. 7-8, pp. 720-725, Febuary 2006.

[4] S. K. Gauri and S. Chakraborty, "Optimization of multiple responses for WEDM processes using weighted principal components," International Journal of Advanced Manufacturing Technology, vol. 40, no. 11-12, pp. 1102-1110, Febuary 2009.

[5] B. C. Routara, S. D. Mohanty, S. Datta, A. Bandopadhyay, and S. S. Mahapatra, "Combined quality loss concept in WPCA-based Taguchi philosophy for optimization of multiple surface quality characteristics of UNS C34000 brass in cylindrical grinding," International Journal of Advanced Manufacturing Technology, vol. 51, no. 1-4, pp. 135-143, March 2010.

[6] A. Biswas, S. Bhaumik, G. Mujumdar, S. Datta, and S. S. Mahapatra, "Bead geometry optimization of submerged arc weld: exploration of weighted principal component analysis," Applied Mechanics and Materials, vol. 110, pp. 790-798, 2012.

Copyright © TAETI

[7] P. C. Padhi, S. S. Mahapatra, S. N. Yadav, and D. K. Tripathi, "Optimization of correlated quality characteristics in WEDM process using Taguchi approach coupled with principal component analysis," Journal of Manufacturing Science and Production, vol. 13, no. 3, pp. 199-208, September 2013.

[8] D. Zhao, Y. Wang, S. Sheng, and Z. Lin, "Multi-objective optimal design of small scale resistance spot welding process with principal component analysis and response surface methodology," Journal of Intelligent Manufacturing , vol. 25, no. 6, pp. 1335-1348, December 2014.

[9] M. K. Das, K. Kumar, T. K. Barman, and P. Sahoo, "Optimization of surface roughness and MRR in EDM using WPCA," Procedia Engineering, vol. 64, pp. 446-455, 2013.

[10] T. B. Rao and A. Gopal Krishna, "Simultaneous optimization of multiple performance characteristics in WEDM for machining ZC63/SiCp MMC," Advances in Manufacturing, vol. 1, no. 3, pp. 265-275, September 2013.

[11] S. K. Gauri and S. Pal, "The principal component analysis (PCA)-based approaches for multi-response optimization: some areas of concerns," International Journal of Advanced Manufacturing Technology, vol. 70, no. 9-12, pp. 1875-1887, February 2014.

[12] B. O. P. Soepangkat and H. C. Kis Agustin, "Multiple performance characteristics optimization in the WEDM process of SKD61 tool steel using Taguchi method combined with weighted principal component analysis (WPCA)," Applied Mechanics and Materials, vol. 758, pp. 21-27, 2015.

[13] S. D. Mohanty, S. S. Mahapatra, and R. C. Mohanty, "Optimization of multiple surface roughness characteristics of electrical discharge machined D2 steel with the help of a tool produced by rapid prototyping using weighted principal component analysis and Taguchi method," Imperial Journal of Interdisciplinary Research, vol. 2, no. 11, pp. 920-927, 2016.

[14] A. Panda, A. K. Sahoo, and A. K. Rout, "Investigations on surface quality characteristics with multi-response parametric optimization and correlations," Alexandria Engineering Journal, vol. 55, no. 2, pp. 1625-1633, June 2016.

[15] N. Lusi, K. Muzaka, and B. O. P. Soepangkat, "Parametric optimization of wire electrical discharge machining process on AISI H13 tool steel using weighted principal component analysis (WPCA) and Taguchi method," ARPN Journal of Engineering and Applied Sciences, vol. 11, no. 2, pp. 945-951, January 2016.

[16] D. M. D. Costa, G. Belinato, T. C. Brito, A. P. Paiva, J. R. Ferreira, and P. P. Balestrassi, "Weighted principal component analysis combined with Taguchi's signal-to-noise ratio to the multi objective optimization of dry end milling process: a comparative study," Journal of the Brazilian Society of Mechanical Sciences and Engineering, vol. 39, no. 5, pp. 1663-1681, May 2017.

[17] A. K. Dhakad and J. Vimal, "Multi response optimization of wire EDM process parameters using Taguchi approach coupled with principal component analysis methodology," International Journal of Engineering, Science and Technology, vol. 9, no. 2, pp. 61-74, 2017.

[18] A. Nair and S. Kumanan, "Multi performance optimization of abrasive water jet machining of Inconel 617 using WPCA," Materials and Manufacturing Processes, vol. 32, no. 6, pp. 693-699, December 2017.

[19] N. Sharma, R. Khanna, and R. D. Gupta, "WEDM process variables investigation for HSLA by response surface methodology and genetic algorithm," Engineering Science and Technology an International Journal, vol. 18, no. 2, pp. 171-177, June 2015.

[20] K. Pearson, "On lines and planes of closest fit RO systems of points in space," Philosophical Magazine, vol. 2, pp. 559-572, 1901.

[21] H. Hotelling, "Analysis of a complex statistical variable into principal components," Journal of Educational Psychology, vol. 24, no. 6, pp. 417-441, 1933.

Copyright © TAETI